Yonago Acta Medica 2022;65(4):296–302 doi: 10.33160/yam.2022.11.005 *Original Article*

Analysis of the Optimum Tapering Angle in Microanastomosis Using Computational Fluid Dynamics

Shunjiro Yagi,* Kento Ikuta,* Shohei Miyazaki,† Ryunosuke Umeda,* Haruka Kanayama,* Mahmoud A. Hifny‡, Maki Morita,* Makoto Nakagaki,* Makoto Tanabe,* Yoshiko Suyama* and Kohei Fukuoka*

**Department of Plastic and Reconstructive Surgery, Tottori University Hospital, Yonago 683-8504, Japan, †Cardio Flow Design, Inc., Chiyoda 102-0082, Tokyo, Japan, and ‡Department of Plastic Surgery, Qena University Hospital, South Valley University, Qena, Egypt*

ABSTRACT

Background In free flap transfer, size discrepancy between the vascular pedicle and recipient vessel can create a problem for microsurgeons and sometimes induces postoperative thrombus formation. When there is a major difference between the diameters of the vascular pedicle and the recipient vessel, the larger vessel is often tapered to perform the anastomosis properly. However, the decision on the tapering angle used depends mostly on the operator's experience. In this study, computational fluid dynamics (CFD) was used to investigate the optimum tapering angle.

Methods Using ANSYS ICEM 16.0 (ANSYS Japan, Tokyo, Japan), simulated vessels of diameters 1.5 mm and 3.0 mm were designed and then used to produce four anastomosis models with the 3.0-mm vessel tapered at angles of 15º, 30º, 60º, and 90º (no tapering). Venous perfusion with a mean value of 13.0 mL/min was simulated, and this was passed through the four anastomosis models in both the forward direction (F), from the smaller to the larger vessel, and the retrograde direction (R), from the larger to the smaller vessel. The velocity, wall shear stress (WSS), and oscillatory shear index (OSI) were measured in these eight patterns and then analyzed using OpenFOAM version 5.

Results The decrease in velocity was limiting. The WSS was greater in the R direction than the F direction at every tapering angle. The OSI also tended to be almost the same in the F direction, and lower at smaller tapering angles in the R direction. And, it was greater in the F direction than in the R direction at every tapering angle. The OSI values for 15º and 30º were almost identical in the R direction.

Conclusion The risk of thrombus formation is thought to be lower when tapering is used for anastomosis if the direction of flow is from the larger to the smaller vessel, rather than vice versa. These results also suggest that the optimum tapering angle is approximately 30º in both directions.

Key words microsurgery; tapering; computational fluid dynamics; size discrepancy; simulation

Free flap transfer is a useful surgical technique for reconstruction in areas including the head and neck, breasts, and limbs reconstruction, and it is now established as a safe surgical procedure.[1, 2] Free skin flap transfer requires microvascular anastomosis, and when the diameters of the vascular pedicle of the flap and of the recipient vessels are different, the tapering technique[3] may be used to resolve this problem. Although it is believed that tapering at a gentler angle enables more natural perfusion, the anastomosis requires a larger number of stitches and thus a longer operating time. How to taper a large vessel is also mostly dependent on the operator's experience. In this study, the optimum tapering angle was investigated by using computational fluid dynamics (CFD) to analyze the flow dynamics of microvascular anastomosis sites created by tapering. Two patterns of microvascular anastomosis, with the blood flowing from a smaller to a larger vessel and vice versa, were also analyzed.

MATERIALS AND METHODS

The simulated vessels were of diameters 1.5 mm and 3.0 mm. The simulated suture thread used for the anastomosis was 0.03 mm in diameter (equivalent to 10-0 nylon). It was passed continuously through the vascular walls at the site of the three-point suture required for tapering.[4] Nine sutures (including the three-point suture) were placed at the anastomosis site, and equally spaced sutures were also placed in the tapered portion. The length of the suture thread protruding into the vascular lumen was 0.115 mm, and its height was 0.0225 mm. A groove of width 0.029 mm and depth 0.029 mm was created in the anastomosis site and the tapered portion (Fig. 1). Computational meshes were created based on ANSYS ICEM16.0 (ANSYS Japan, Tokyo, Japan). Four different models were created, with the tapering

Corresponding author: Shunjiro Yagi, MD, PhD
yagishun68@gmail.com
Received 2022 September 30
Accepted 2022 October 25
Online published 2022 November 28
Abbreviations: CFD, computational fluid dynamics; F, forward direction; OSI, oscillatory shear index; R, retrograde direction; WSS, wall shear stress

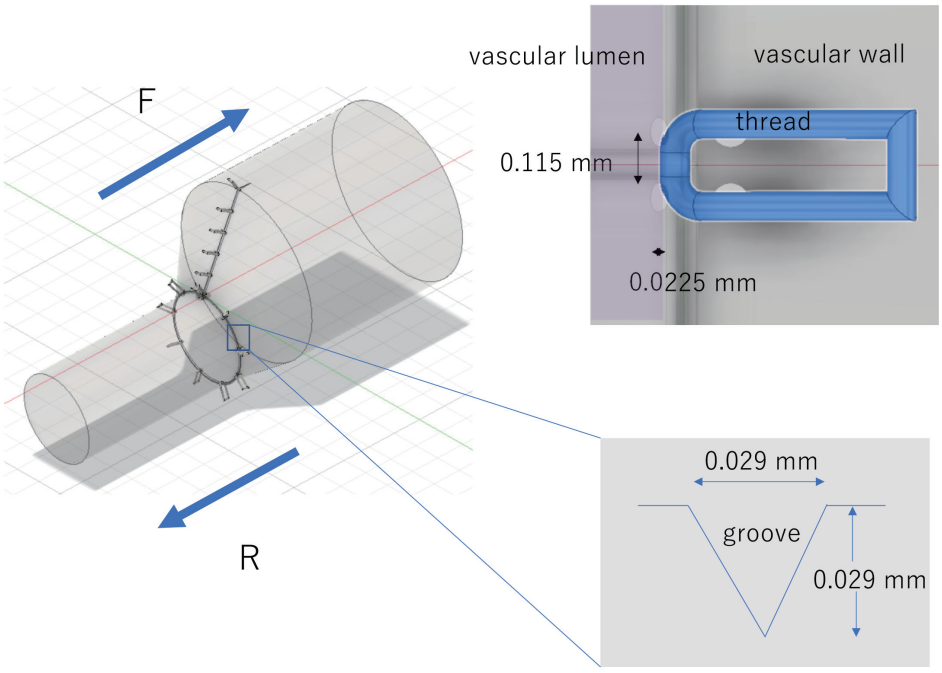

Fig. 1. Vascular anastomosis model. Sutures are placed at nine points at the anastomosis site, including a three-point suture. Sutures are also placed in the tapered portion at the same intervals as in the anastomosis. The diameter of the suture thread is 0.03 mm. The length of the suture thread protruding into the vascular lumen is 0.115 mm, and its height is 0.0225 mm. A groove of width 0.029 mm and depth 0.029 mm is created in the anastomosis site and the tapered portion. F, Forward direction, from the smaller to the larger vessel; R, Retrograde direction, from the larger to the smaller vessel.

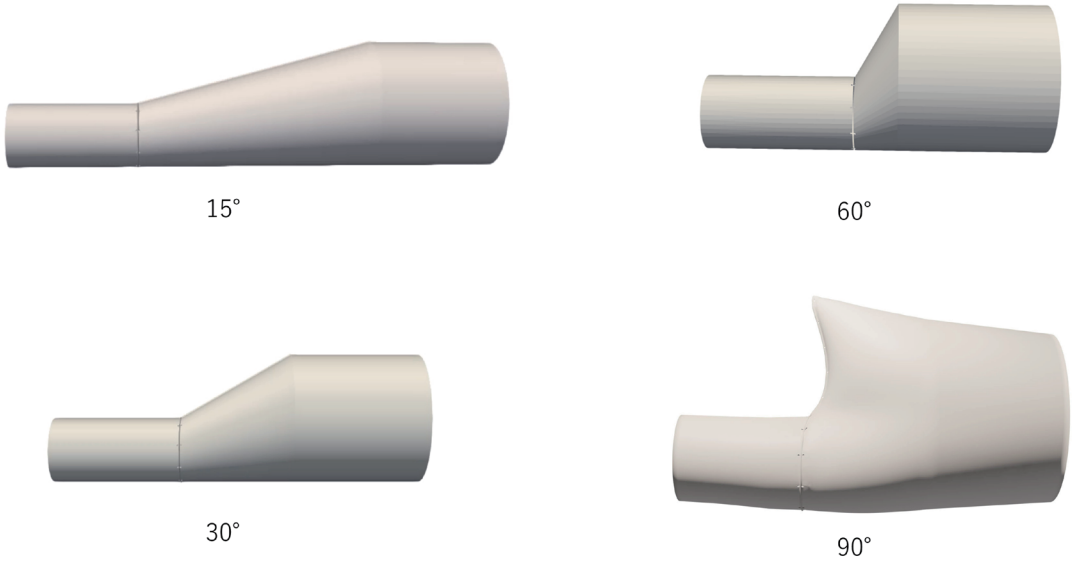

Fig. 2. Models with tapering at 15°, 30°, 60°, and 90°.

angle of the 3.0-mm-diameter vessel being 15°, 30°, 60°, or 90° (no tapering) (Fig. 2). The mesh consisted of 1,585,649 elements and 434,492 nodes at 15°, 1,059,769 elements and 372,645 nodes at 30°, 1,598,761 elements and 294,929 nodes at 60°, and 722,662 elements and 201,394 nodes at 90°.

Inlet blood flow into the anastomosis site and the tapered vessel was simulated on the basis of the venous perfusion measured by an ultrasound flowmeter (HT323 surgical flowmeter, Transonic Systems, Ithaca, NY).[5]

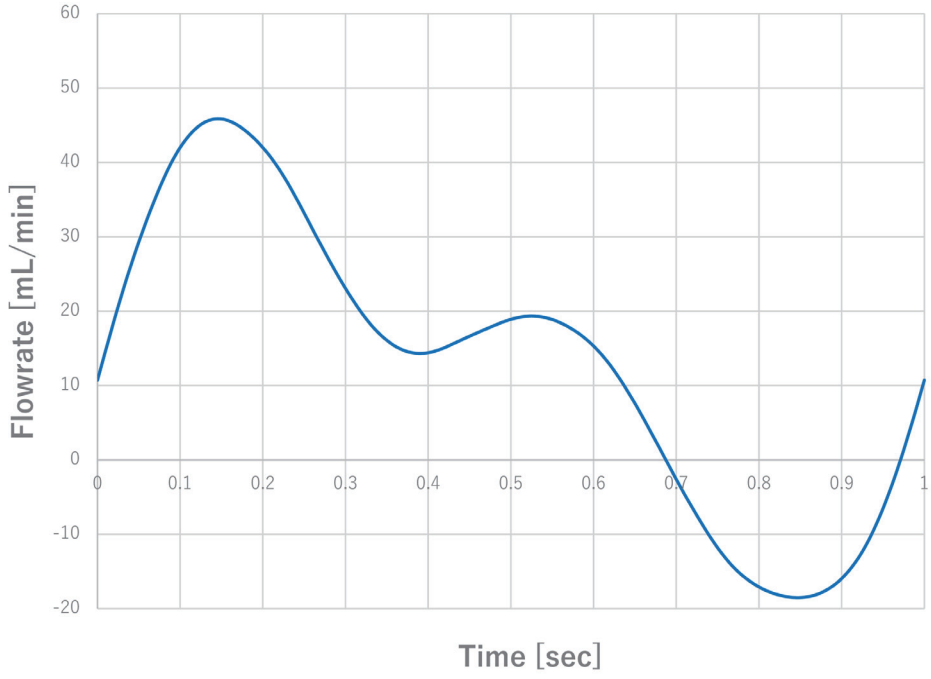

Fig. 3. Model venous perfusion. This is set so that the minimum value is –19 mL/min at 0.84 s, and the maximum value is 45 mL/min at 0.14 s. The mean value is 13 mL/min, and 1 cycle lasts for 1 s.

This model venous perfusion had a minimum value of –19 mg/min at 0.84 s, a maximum value of 45 mL/min at 0.14 s, and a mean value of 13 mL/min, with 1 cycle lasting 1 s (Fig. 3). The density of the venous blood was set to 1,060 kg/m^3, and its coefficient of viscosity to 0.004 Pa-s.[6, 7] The pressure gradient at the outlet was set to zero, and the wall surface was given a no-slip condition. The CFD analysis conditions were as follows. OpenFOAM v5.0 software was used for the analysis. Turbulent pulsatile flow simulation was performed with reference to previous hemodynamic research, as follows. The software solved the Navier–Stokes equations of an incompressible transient Newtonian fluid. Time step size was set to 5.0 times 10^{-5} seconds to reduce the Courant number to the sufficient level. The convergence criteria were set to 10-5, which times the residual at each time step.

Simulated perfusion was passed through the four vascular anastomosis models with 15º–90º tapering in the forward direction (F), from the smaller to the larger vessel, and in the retrograde direction (R), from the larger to the smaller vessel. Perfusion with a velocity of < 0.01 m/s in the area around the anastomosis was visualized for a total of eight patterns (15F, 30F, 60F, 90F, 15R, 30R, 60R, and 90R). Wall shear stress (WSS) and the oscillatory shear index (OSI) were also analyzed. CFD postprocessing software (ParaView, Kitware, NY) was used for these analyses. The WSS is calculated from the tangential component of the blood flow velocity gradient at the vessel wall and the blood viscosity. In other words, it is the frictional force exerted by the blood on the vascular wall measured in Pa (N/m2).[8] The OSI expresses the size of the changes in direction and magnitude of the WSS. It thus indicates the degree of reversing direction of the WSS within a single pulse cycle as

$$\mathrm{OSI} = \frac{1}{2}\left(1 - \frac{\left|\int_0^T \mathbf{WSS}\, dt\right|}{\int_0^T |\mathbf{WSS}|\, dt}\right)$$

where, T is one cardiac time, WSS is wall shear stress vector.[9]

RESULTS

Velocity

In all simulated vessels, a decrease in velocity was evident around the suture thread protruding into the vascular lumen, but this did not cause major turbulence. In the 15º models, in both the F and R directions, the blood flow velocity slowed at the anastomosis site and along the groove where the tapered vessel was sutured. In the 30º, and 60º models, in both the F and R directions, a decrease in blood flow was evident around the groove at the anastomosis site and at the locations of

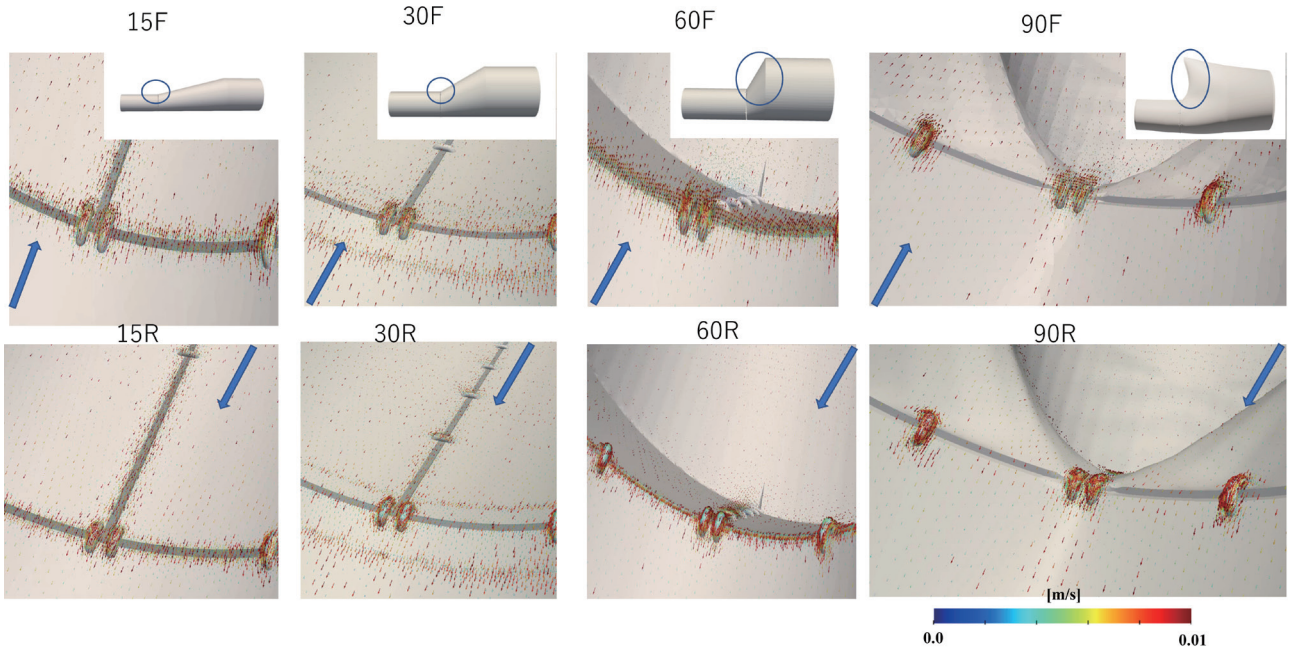

Fig. 4. Visualization of velocity. Vectors of < 0.01 m/s are displayed. The arrows indicate the direction of flow.

sutures around the anastomosis site (Fig. 4).

Wall shear stress

The maximum WSS value was 53.9 Pa for the 15F pattern, 84.9 Pa for 15R, 47.1 Pa for 30F, and 125.0 Pa for 30R, 42.2 Pa for the 60F pattern, 178.5 Pa for 60R, 21.5 Pa for 90F, and 126.7 Pa for 90R, each recorded at 0.15 s when the perfusion was greatest. In all models, the maximum WSS was observed near the peak of the suture thread at the anastomosis site (Fig. 5).

Oscillatory shear index

The local maximum OSI value recorded was 0.50 for the 15F pattern, 0.22 for 15R, 0.49 for 30F, 0.22 for 30R, 0.47 for 60F, 0.35 for 60R, 0.47 for 90F, and 0.39 for 90R. For all tapering angles, the OSI was higher in the F direction than in the R direction. For the 15F pattern, the site of the local maximum OSI value was along the groove at the suture site where the vessel was tapered. For the 30F pattern, the sites of the local maximum OSI value were at the base of the suture thread of the three-point suture and along the vascular wall on its distal side. For the 60F and 90F patterns, the site of the local maximum OSI value was at the suture thread of the three-point suture and along the groove at the vascular anastomosis. For 60F, 60R, 90F and 90R, the OSI was also high at the tip of the tapered portion. In the R direction, the OSI was high at the base of the suture thread of the three-point suture for every angle (Fig. 6).

DISCUSSION

Improvements in computer function and advances in simulation techniques have allowed the application of CFD techniques to the analysis of blood flow. The use of blood flow analysis by CFD to assess the risk of cerebral aneurysm rupture has been widely reported.[10–12] Other studies have described the value of CFD for microvascular anastomoses,[4, 5, 13] but the present study is the first to focus on investigating the optimum tapering angle.

Visualization at a velocity of < 0.01 m/s around the anastomosis site showed that the velocity was decreased by the sutures used in the anastomosis. Although the risk of thrombus formation cannot simply be predicted from this decrease in velocity alone, if the suture is loosely tied or blood flow is generated by a suture thread, this might conceivably induce thrombus formation. In the area around the sutures used in tapering, sutures closer to the anastomosis site did decrease the velocity somewhat, but those more distant from the anastomosis site had little effect in slowing the velocity. This suggested that, although more suture thread was used for tapering at smaller tapering angles, this increase in the amount of suture thread had almost no effect in reducing blood flow.

WSS is known to inhibit thrombus formation.[14] WSS is a stress that acts tangentially to the blood vessel, and should a thrombus form near the peak of the suture thread, where the WSS is high, it would immediately be detached by the blood flow, making it more difficult for

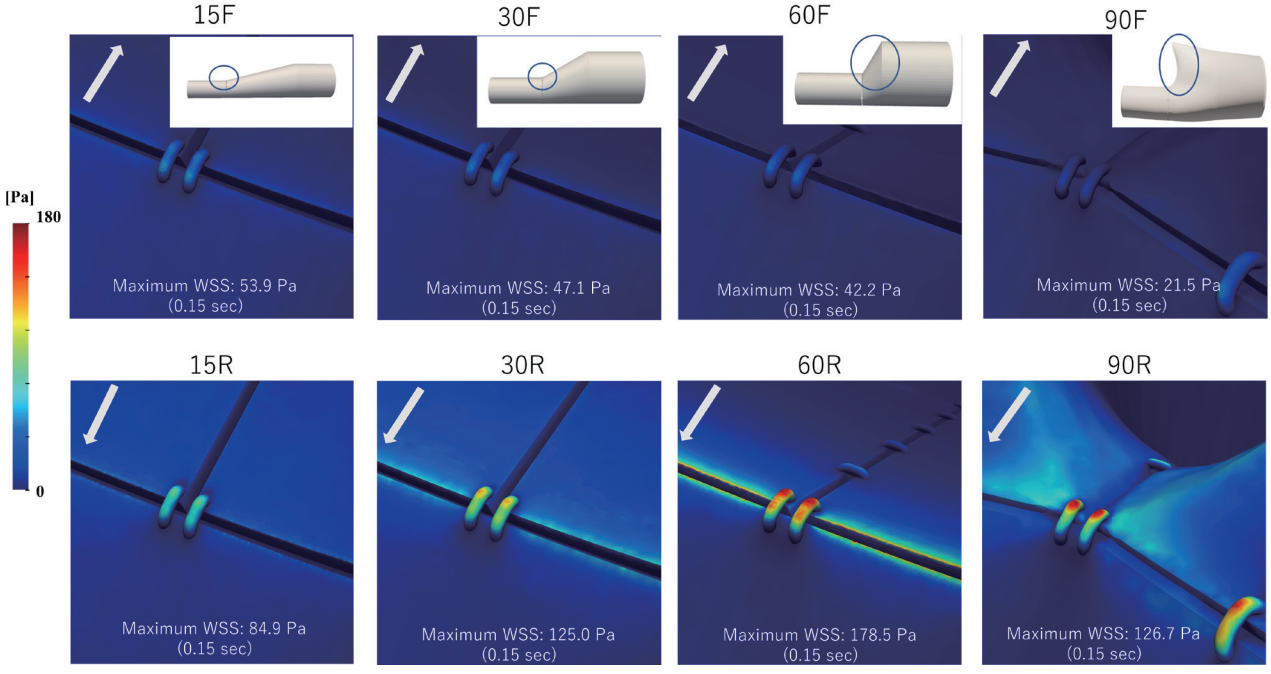

Fig. 5. Wall shear stress (WSS). In every model, the maximum WSS is near the peak of the suture thread at the anastomosis site. The arrows indicate the direction of flow.

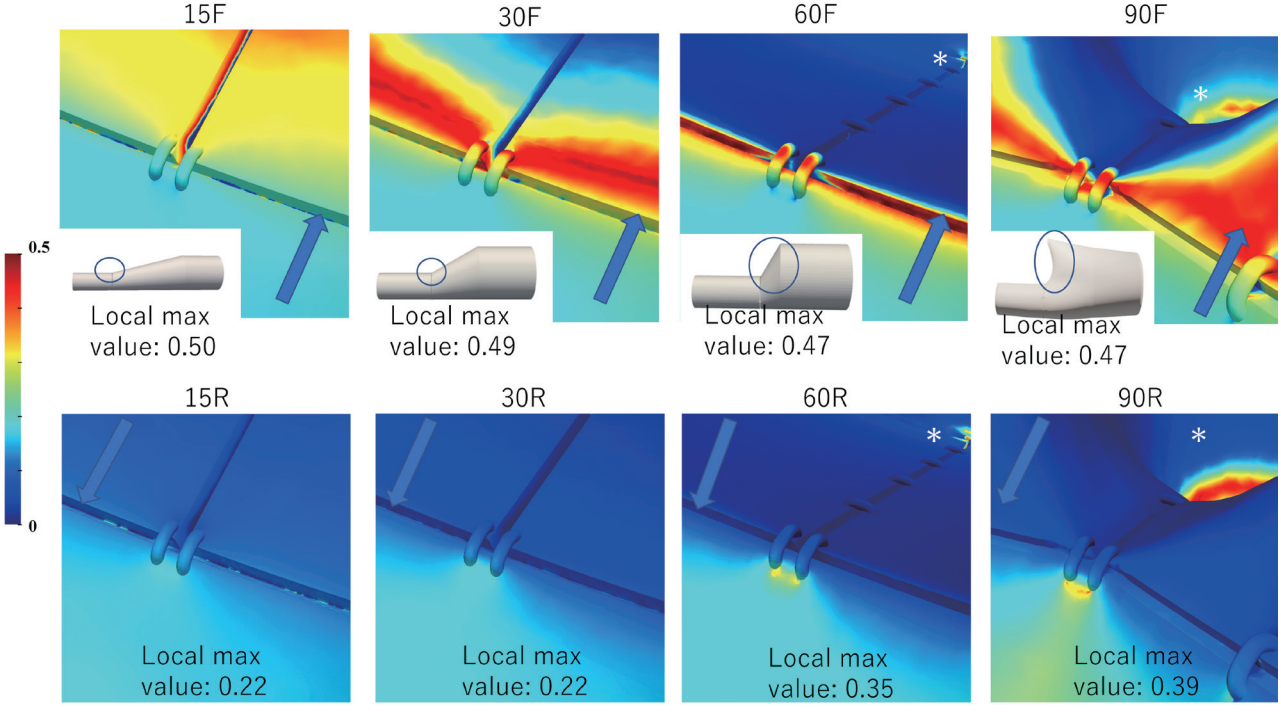

Fig. 6. Oscillatory shear index (OSI). The arrows show the direction of flow. For the 60F pattern, the site of the local maximum OSI value is at the peak of the suture thread of the three-point suture and along the vascular anastomosis. For the 60F, 90F, and 60R, 90R patterns, the OSI is also high at the tip of the tapered portion (*).

thrombus formation to occur.

The highest WSS value in every pattern was recorded near the peak of the suture thread. Although the suture thread contributed to decreasing blood flow, we suppose the magnitude of the shear force near the suture thread acts to hinder thrombus formation. At every angle, the WSS value was higher in the R direction than in the F direction, suggesting that although the stress on the anastomosis site was greater in the R direction, thrombus formation was less likely to occur.

The OSI, another important CFD index, was also analyzed. A high OSI is believed to cause the generation of active oxygen species.[15] Vascular endothelial cells suffer severe oxidative stress during post-ischemic reperfusion, and vascular endothelial cell damage caused by active oxygen species is likely to be involved in thrombus formation.[16–18]

In the simulations in the present study, a higher OSI was recorded in the F direction than in the R direction at every angle. Although many surgeons may believe that the risk of thrombus formation is normally increased when a larger vessel is joined to a smaller vessel in the creation of a microvascular anastomosis, the results of the present simulation showed the opposite. This may have been because venous perfusion was modeled, which includes a retrograde flow for some time. In the F direction, when the blood is flowing in the antegrade direction, the flow separation[19] results in an area of reduced flow along the tapered portion compared with the amount of blood flowing in, whereas when the blood is flowing in the retrograde direction, the blood flows directly along the tapered portion, both increasing the difference in the WSS and increasing the OSI.

For the 15R and 30R patterns, the OSI values recorded were almost identical. This suggests that, during a vascular anastomosis in the R direction, a 30º tapering angle may be ideal. There is also a site of locally high OSI at the base of the suture thread forming the three-point suture in the R direction. However, the OSI values for every angle were lower than those for the F direction, suggesting that, in terms of fluid mechanics, tapering in the R direction entails a lower risk of thrombus formation than does tapering in the F direction.

For all F direction patterns OSI values are the OSI values recorded were almost same. And, for the 60F and 90F patterns, high OSI values were recorded at the peak of the three-point suture. The flow velocity also decreased at this site, placing it at increased risk of thrombus formation. This suggests that a tapering angle of 30º or less may be required in the F direction. As seen for the 60F, 90F, and 60R, 90R patterns, sites recording a high OSI are also present at the peaks where the large vessel is sewn together, and the 90F pattern had the highest risk of thrombus formation.

Because postoperative thrombus formation tends to occur more frequently at venous anastomoses than at arterial anastomoses,[20] a model venous waveform was used in our CFD analysis. Differences between venous flow and arterial flow are that arterial flow volume is larger than venous one and that arterial blood flows only in antegrade direction. So, it is expected that OSI in arterial anastomoses is lower than venous anastomoses. This may be one reason that thrombus formation is more likely to occur at venous anastomoses than at arterial anastomoses in microvascular anastomoses.

CFD analysis is useful from the viewpoint of animal protection, as no experimental animals are used. However, one limitation of this study is that it is difficult to recreate *in vivo* conditions exactly by CFD. Consistency between the calculated values and actual measured values is extremely important in CFD analysis, but when applying CFD analysis *in vivo*, validation experiments are highly problematic. This issue can be resolved by adding further conditions to diminish the gap between CFD results and real-world clinical practice. Other problems include the treatment of the simulated blood vessels as rigid bodies. To enable a closer approximation of reality will require the incorporation of detailed patient or individual vascular data into the conditions used. Although it is technically complex, the use of fluid structural interaction (FSI), which analyzes blood vessels as elastic bodies that change shape depending on the amount of blood flowing through them,[21, 22] may resolve this issue.

In conclusion, CFD was used to conduct blood flow analysis of microvascular anastomoses created by tapering. The present results suggest that the risk of thrombus formation is lower when blood flows from a larger to a smaller vessel than when it flows from a smaller vessel to a larger one in venous microvascular anastomoses. They also suggested that the optimum tapering angle may be approximately 30º in both the F and R directions.

The authors declare no conflict of interest.

REFERENCES

1 Yagi S, Kamei Y, Nakayama B, Toriyama K, Torii S. A new design for free flap reconstruction of the tongue and oropharynx. J Reconstr Microsurg. 2008;24:211-9. DOI: 10.1055/s-2008-1078691, PMID: 18491260

2 Kamei Y, Toriyama K, Yagi S, Takanari K, Torii S. Analysis of 13 cases with gastroepiploic vessels used as grafts. J Reconstr Microsurg. 2008;24:515-8. DOI: 10.1055/s-0028-1088234, PMID: 18798143

3 Ryan AD, Goldberg I, O'Brien, MacLeod AM. Anastomosis of vessels of unequal diameter using an interpositional vein graft. Plast Reconstr Surg. 1988;81:414-7. DOI: 10.1097/00006534-198803000-00018, PMID: 3340676

4 Yagi S, Sasaki T, Fukuhara T, Fujii K, Morita M, Fukuoka K, et al. Hemodynamic analysis of a three-point suture during tapering technique for microanastomosis using computational fluid dynamics. J Craniofac Surg. 2021;32:2749-52. DOI: 10.1097/SCS.0000000000007859, PMID: 34238882

5 Yagi S, Sasaki T, Fukuhara T, Fujii K, Morita M, Suyama Y, et al. Hemodynamic analysis of a microanastomosis using computational fluid dynamics. Yonago Acta Med. 2020;63:308-12. DOI: 10.33160/yam.2020.11.013, PMID: 33253341

6 Itatani K, Miyaji K, Qian Y, Liu JL, Miyakoshi T, Murakami A, et al. Influence of surgical arch reconstruction methods on single ventricle workload in the Norwood procedure. J Thorac Cardiovasc Surg. 2012;144:130-8. DOI: 10.1016/j.jtcvs.2011.08.013, PMID: 21907359

7 Miyazaki S, Miyaji K, Itatani K, Oka N, Goto S, Nakamura M, et al. Surgical strategy for aortic arch reconstruction after the Norwood procedure based on numerical flow analysis. Interact Cardiovasc Thorac Surg. 2018;26:460-7. DOI: 10.1093/icvts/ivx332, PMID: 29049796

8 Malek AM, Alper SL, Izumo S. Hemodynamic shear stress and its role in atherosclerosis. JAMA. 1999;282:2035-42. DOI: 10.1001/jama.282.21.2035, PMID: 10591386

9 He X, Ku DN. Pulsatile flow in the human left coronary artery bifurcation: average conditions. J Biomech Eng. 1996;118:74-82. DOI: 10.1115/1.2795948, PMID: 8833077

10 Cebral JR, Mut F, Weir J, Putman C. Quantitative characterization of the hemodynamic environment in ruptured and unruptured brain aneurysms. AJNR Am J Neuroradiol. 2011;32:145-51. DOI: 10.3174/ajnr.A2419, PMID: 21127144

11 Cebral JR, Vazquez M, Sforza DM, Houzeaux G, Tateshima S, Scrivano E, et al. Analysis of hemodynamics and wall mechanics at sites of cerebral aneurysm rupture. J Neurointerv Surg. 2015;7:530-6. DOI: 10.1136/neurintsurg-2014-011247, PMID: 24827066

12 Omodaka S, Sugiyama S, Inoue T, Funamoto K, Fujimura M, Shimizu H, et al. Local hemodynamics at the rupture point of cerebral aneurysms determined by computational fluid dynamics analysis. Cerebrovasc Dis. 2012;34:121-9. DOI: 10.1159/000339678, PMID: 22965244

13 Wain RAJ, Whitty JPM, Dalal MD, Holmes MC, Ahmed W. Blood flow through sutured and coupled microvascular anastomoses: A comparative computational study. J Plast Reconstr Aesthet Surg. 2014;67:951-9. DOI: 10.1016/j.bjps.2014.03.016, PMID: 24731801

14 Maruyama O, Kosaka R, Nishida M, Yamane T, Tatsumi E, Taenaka Y. In vitro thrombogenesis resulting from decreased shear rate and blood coagulability. Int J Artif Organs. 2016;39:194-9. DOI: 10.5301/ijao.5000496, PMID: 27199137

15 Hwang J, Saha A, Boo YC, Sorescu GP, McNally JS, Holland SM, et al. Oscillatory shear stress stimulates endothelial production of O2- from p47phox-dependent NAD(P)H oxidases, leading to monocyte adhesion. J Biol Chem. 2003;278:47291-8. DOI: 10.1074/jbc.M305150200, PMID: 12958309

16 Kietadisorn R, Juni RP, Moens AL. Tackling endothelial dysfunction by modulating NOS uncoupling: new insights into its pathogenesis and therapeutic possibilities. Am J Physiol Endocrinol Metab. 2012;302:E481-95. DOI: 10.1152/ajpendo.00540.2011, PMID: 22167522

17 den Hengst WA, Gielis JF, Lin JY, Van Schil PE, De Windt LJ, Moens AL. Lung ischemia-reperfusion injury: a molecular and clinical view on a complex pathophysiological process. Am J Physiol Heart Circ Physiol. 2010;299:H1283-99. DOI: 10.1152/ajpheart.00251.2010, PMID: 20833966

18 Moens AL, Claeys MJ, Timmermans JP, Vrints CJ. Myocardial ischemia/reperfusion-injury, a clinical view on a complex pathophysiological process. Int J Cardiol. 2005;100:179-90. DOI: 10.1016/j.ijcard.2004.04.013, PMID: 15823623

19 Kertzscher U, Goubergrits L, Affeld K. Flow separations in blood flow—its significance in the human circulation system and in artificial organs [Internet]. Southampton: WIT Press; 2022 [cited 2022 Aug 8]. Available from: https://www.witpress.com/Secure/elibrary/papers/1845640950/18456409 50508FU2.pdf

20 Suh JM, Chung CH, Chang YJ. Head and neck reconstruction using free flaps: a 30-year medical record review. Arch Craniofac Surg. 2021;22:38-44. DOI: 10.7181/acfs.2020.00745, PMID: 33714251

21 Lee CJ, Zhang Y, Takao H, Murayama Y, Qian Y. A fluid–structure interaction study using patient-specific ruptured and unruptured aneurysm: the effect of aneurysm morphology, hypertension and elasticity. J Biomech. 2013;46:2402-10. DOI: 10.1016/j.jbiomech.2013.07.016, PMID: 23962529

22 Valencia A, Burdiles P, Ignat M, Mura J, Bravo E, Rivera R, et al. Fluid structural analysis of human cerebral aneurysm using their own wall mechanical properties. Comput Math Methods Med. 2013;2013:1-18. DOI: 10.1155/2013/293128, PMID: 24151523